Cholesterol Organization in Membranes at Low Concentrations: Effects of Curvature Stress and Membrane Thickness

R. Rukmini, Satinder S. Rawat, Samares C. Biswas, and Amitabha Chattopadhyay
Centre for Cellular & Molecular Biology, Hyderabad 500 007, India

ABSTRACT Cholesterol is often found distributed nonrandomly in domains in biological and model membranes and has been reported to be distributed heterogeneously among various intracellular membranes. Although a large body of literature exists on the organization of cholesterol in plasma membranes or membranes with high cholesterol content, very little is known about organization of cholesterol in membranes containing low amounts of cholesterol. Using a fluorescent cholesterol analog (25-[*N*-[(7-nitrobenz-2-oxa-1,3-diazol-4-yl)-methyl]amino]-27-norcholesterol, or NBD-cholesterol), we have previously shown that cholesterol may exhibit local organization even at very low concentrations in membranes, which could possibly be attributable to transbilayer tail-to-tail dimers. This is supported by similar observations reported by other groups using cholesterol or dehydroergosterol, a naturally occurring fluorescent cholesterol analog which closely mimics cholesterol. In this paper, we have tested the basic features of cholesterol organization in membranes at low concentrations using spectral features of dehydroergosterol. More importantly, we have investigated the role of membrane surface curvature and thickness on transbilayer dimer arrangement of cholesterol using NBD-cholesterol. We find that dimerization is not favored in membranes with high curvature. However, cholesterol dimers are observed again if the curvature stress is relieved. Further, we have monitored the effect of membrane thickness on the dimerization process. Our results show that the dimerization process is stringently controlled by a narrow window of membrane thickness. Interestingly, this type of local organization of NBD-cholesterol at low concentrations is also observed in sphingomyelin-containing membranes. These results could be significant in membranes that have very low cholesterol content, such as the endoplasmic reticulum and the inner mitochondrial membrane, and in trafficking and sorting of cellular cholesterol.

INTRODUCTION

Cholesterol is a major constituent of eukaryotic membranes and plays a crucial role in membrane organization, dynamics, function and sorting (Yeagle, 1985; Liscum and Underwood, 1995; Schroeder et al., 1996; Fielding and Fielding, 1997; Liscum and Munn, 1999; Simons and Ikonen, 2000). The role of cholesterol in signal transduction is being increasingly recognized (Incardona and Eaton, 2000). It has recently been implicated in embryonic development in *Drosophila* (Porter et al., 1996), and programmed cell death (Maccarrone et al., 1998). It also serves as a precursor for the synthesis of steroid hormones, bile acids, and lipoproteins. Cellular levels of cholesterol and its compartmentalization into different organelles are stringently controlled, and defects in its trafficking pathway have been shown to give rise to metabolic storage diseases such as Niemann-Pick type C (Mukherjee and Maxfield, 1999). Cholesterol is often found distributed nonrandomly in domains in biological and model membranes (Liscum and Underwood, 1995; Mukherjee and Chattopadhyay, 1996; Schroeder et al., 1995, 1996; Simons and Ikonen, 1997, 2000; Xu and London, 2000) and has been shown to preferentially interact with a subset of membrane lipids (McMullen and McElhaney, 1996) or proteins (Gimpl et al., 1997). Indeed, structurally and kinetically distinct cholesterol-rich and -poor domains have been detected in cellular membranes (Schroeder et al., 1991). Dynamic clustering of cholesterol (along with other membrane components such as sphingolipids) has given rise to the idea of specialized microdomains or "rafts" in the cell membrane that might play crucial roles in cellular functions such as signal transduction, adhesion, motility, and sorting and trafficking of membrane components (Simons and Ikonen, 1997, 2000). In addition, cholesterol has been reported to be distributed heterogeneously among various intracellular membranes. For example, along the biosynthetic route, the lowest cholesterol concentration is found in the membranes of the endoplasmic reticulum (ER), which, interestingly, is the site of cholesterol biosynthesis (Bretscher and Munro, 1993). Cholesterol concentration increases progressively along the *cis*-, *medial*-, and *trans*-Golgi stacks (Bretscher and Munro, 1993), whereas the highest concentration (~90% of the total cellular cholesterol) is found in the plasma membrane (Lange et al., 1989).

Although a large body of literature exists on the organization of cholesterol in plasma membranes or membranes with high cholesterol content, very little is known about its organization in the membrane when the cholesterol content is very low (< 5 mol %), similar to what is found in ER and inner mitochondrial membranes (Lange et al., 1999). We have previously shown, using a fluorescent analog of cholesterol

Received for publication 21 April 2000 and in final form 12 June 2001.

Address reprint requests to Amitabha Chattopadhyay, Centre for Cellular & Molecular Biology, Uppal Road, Hyderabad 500 007, India. Tel.: 91-40-7172241; Fax: 91-40-7171195; E-mail: amit@ccmb.ap.nic.in.

Dr. Rawai's present address is Room 211, Building 469, Laboratory of Experimental and Computational Biology, NCI-FCRDC, National Institutes of Health, Frederick, MD 21702-1201.

Dr. Biswas' present address is Institut National de la Recherche Agronomique, Unité de Biochimie et Technologie des Proteines, Rue de la Géraudière, BP 71627, 44316 Nantes Cedex 03, France

0006-3495/01/10/2122/13 $2.00

(25-[*N*-[(7-nitrobenz-2-oxa-1,3-diazol-4-yl)-methyl]amino]-27-norcholesterol, or NBD-cholesterol) in which the flexible acyl chain of cholesterol is labeled with the NBD group, that cholesterol may exhibit local organization even at very low concentrations in membranes. Our results indicated the possible presence of transbilayer tail-to-tail dimers of cholesterol in such membranes (Mukherjee and Chattopadhyay, 1996). This is supported by similar observations reported by other groups obtained under comparable cholesterol concentrations (Harris et al., 1995; Loura and Prieto, 1997).

Fluorescent sterols offer a powerful approach for monitoring cholesterol organization and dynamics in membranes because of their high sensitivity, time resolution, and multiplicity of measurable parameters (Schroeder, 1984; Grechishnikova et al., 1999). Sterols covalently linked to extrinsic fluorophores are commonly used for such studies. The advantage with this approach is that one has a choice of the fluorescent label to be used and, therefore, specific probes with appropriate characteristics can be designed for specific applications. A widely used extrinsic fluorophore in biophysical, biochemical, and cell biological studies is the NBD group (Chattopadhyay, 1990). NBD-labeled lipids are extensively used as fluorescent analogs of native lipids in biological and model membranes to study a variety of processes (Kobayashi and Pagano, 1988; Chattopadhyay, 1990; Mazeres et al., 1996; Liao et al., 1997; Chattopadhyay and Mukherjee, 1999).

The NBD moiety possesses some of the most desirable properties for serving as an excellent probe for both spectroscopic and microscopic applications. It is very weakly fluorescent in water. Upon transfer to a hydrophobic medium, it fluoresces brightly in the visible range and exhibits a high degree of environmental sensitivity (Chattopadhyay and London, 1988; Lin and Struve, 1991; Chattopadhyay and Mukherjee, 1993; Fery-Forgues et al., 1993; Mukherjee et al., 1994). Fluorescence lifetime of the NBD group is extremely sensitive to the environmental polarity (Lin and Struve, 1991; Rawat and Chattopadhyay, 1999). It is relatively photostable, and lipids labeled with the NBD group mimic endogenous lipids in studies of intracellular lipid transport (van Meer et al., 1987; Koval and Pagano, 1990).

A detailed characterization of the spectroscopic and ionization properties as well as the specific location of NBD-cholesterol in membranes has earlier been carried out by one of us (Chattopadhyay and London, 1987, 1988). In model membrane systems, the NBD group of NBD-cholesterol has been found to be localized deep in the hydrocarbon region of the membrane, approximately 5–6 Å from the center of the bilayer (Chattopadhyay and London, 1987, 1988; Mukherjee and Chattopadhyay, 1996). Unlike the NBD-labeled phospholipids, the NBD group in NBD-cholesterol does not loop back to the membrane interface despite its polar nature, probably because of the stereochemical rigidity of the sterol ring (Chattopadhyay, 1990). This unique orientation of NBD-cholesterol offers a convenient handle for localization of a polar and potentially reactive group deep inside the membrane. The unique position of this probe in the membrane has been previously exploited in a fluorescence resonance energy transfer study of the spatial relationships of specific sites on chloroplast coupling factor to the membrane surface in reconstituted vesicles (Mitra and Hammes, 1990). A closely related analog of this probe in which the NBD group is attached to a shorter alkyl chain (known as fluoresterol) has recently been shown to faithfully mimic the biochemistry and cell biology of intestinal cholesterol absorption (Sparrow et al., 1999). When given orally to hamsters, it was taken up into plasma, and the uptake was blocked by compounds that block cholesterol absorption. In addition, fluoresterol was shown to be esterified both in vivo and in vitro (in cultured cells), indicating that it was able to traffic to the ER and act as a substrate for acyl CoA cholesterol acyltransferase, the enzyme that esterifies native cholesterol. Thus, NBD-labeled cholesterol analogs represent a useful class of molecules that mimic native cholesterol properties in vitro and in vivo.

In this paper, we have investigated the role of membrane surface curvature and thickness on transbilayer dimerization occurring at low concentrations of cholesterol using NBD-cholesterol as a fluorescent cholesterol analog. Our results show that the transbilayer dimer arrangement of cholesterol observed at low concentrations in membranes (Harris et al., 1995; Mukherjee and Chattopadhyay, 1996; Loura and Prieto, 1997) is sensitive to the membrane surface curvature and that cholesterol dimerization is not favored in membranes with high surface curvature. However, if the curvature stress is relieved by regenerating large vesicles, cholesterol dimers are observed again indicating the reversible modulation of the monomer/dimer equilibrium by membrane surface curvature. Further, we have examined the effect of membrane thickness on the dimerization process using NBD-cholesterol fluorescence. Our results indicate that cholesterol dimers are formed in dipalmitoyl-*sn*-glycero-3-phosphocholine (DPPC) and dimyristoyl-*sn*-glycero-3-phosphocholine (DMPC) membranes in the gel phase, but not in distearoyl-*sn*-glycero-3-phosphocholine (DSPC) and diarachidoyl-*sn*-glycero-3-phosphocholine (DAPC) membranes which are thicker membranes because of longer fatty acyl chains. Likewise, cholesterol dimers are not detected in the relatively thin dilauroyl-*sn*-glycero-3-phosphocholine (DLPC) membranes. Thus, it seems that the dimerization process is stringently controlled by a narrow window of membrane thickness. We also show that some of the basic features of cholesterol organization in membranes at low concentrations obtained using NBD-cholesterol are in agreement with concentration-dependent changes observed in spectral features (peak intensity ratios) of dehydroergosterol ($\Delta^{5,7,9(11)22}$-ergostatetraen-3β-ol, or DHE), a naturally occurring fluorescent cholesterol analog which closely mimics cholesterol.

MATERIALS AND METHODS

Materials

DPPC, DMPC, and DHE were obtained from Sigma Chemical Co. (St. Louis, MO). DLPC, DSPC, DAPC, and brain sphingomyelin were from Avanti Polar Lipids (Birmingham, AL). NBD-cholesterol was from Molecular Probes (Eugene, OR). Lipids were checked for purity by thin-layer chromatography on precoated silica gel plates (Sigma) in chloroform/methanol/water (65:35:5, v/v) and were found to give only one spot in all cases with a phosphate-sensitive spray and on subsequent charring (Dittmer and Lester, 1964). Thin-layer chromatography of NBD-cholesterol was done using the same solvents but in a slightly different proportion (65:35:4, v/v), and it was found to be pure when detected by its color or fluorescence (Mukherjee and Chattopadhyay, 1996). The concentrations of the phospholipids were determined by phosphate assay subsequent to total digestion by perchloric acid (McClare, 1971). DMPC was used as an internal standard to assess lipid digestion. The concentration of NBD-cholesterol and DHE in methanolic stock solutions were calculated from their respective molar extinction coefficients (ϵ) of 22,000 M^{-1} cm^{-1} at 484 nm (Chattopadhyay and Mukherjee, 1999) and 10,500 M^{-1} cm^{-1} at 324 nm (Smutzer et al., 1986). All other chemicals used were of the highest purity available. Solvents used were of spectroscopic grade. Water was purified through a Millipore (Bedford, MA) Milli-Q system and used throughout.

Sample preparations

Experiments in which the membrane surface curvature was changed were done with different types of vesicles of DPPC containing 2.0 mol % NBD-cholesterol. Samples containing 640 nmol (1280 nmol for time-resolved fluorescence measurements) of DPPC and 12.8 nmol (25.6 nmol for time-resolved fluorescence measurements) of NBD-cholesterol were taken together in methanol, a few drops of chloroform were added and mixed well, and dried under a stream of nitrogen while being warmed gently (~35°C). After the lipids were dried further under a high vacuum for at least 3 h, they were hydrated (swelled) by adding 1.5 ml of 10 mM sodium phosphate, 150 mM sodium chloride, pH 7.2 buffer, and vortexed for 3 min to disperse the lipid and form homogeneous multilamellar vesicles. The buffer was always maintained at a temperature well above the phase transition temperature of DPPC (i.e., >41°C) as the vesicles were made. Large unilamellar vesicles (LUVs) of 100-nm diameter were then prepared by the extrusion technique using an Avestin Liposofast Extruder (Ottawa, Ontario, Canada) as previously described (MacDonald et al., 1991). Briefly, the multilamellar vesicles of DPPC were freeze-thawed five times using liquid nitrogen to ensure solute equilibration between trapped and bulk solutions, and then extruded through polycarbonate filters (pore diameter of 100 nm) mounted in the extruder fitted with Hamilton syringes (Hamilton Company, Reno, NV). The samples were subjected to 17 passes through the polycarbonate filter to give the final LUV suspension. Samples were kept overnight in dark at room temperature for equilibration before making measurements. For experiments involving DHE, LUVs of DPPC containing various concentrations of DHE were prepared the same way. For experiments in which sphingomyelin was used, LUVs of DPPC/sphingomyelin (70:30, mol/mol) containing various concentrations of NBD-cholesterol were also prepared this way.

Small unilamellar vesicles (SUVs) were generated from LUVs (after fluorescence and/or absorbance measurements were made) by sonication till clarity using a Branson model 250 sonifier (Branson Ultrasonics, Dansbury, CT) fitted with a microtip. The sonicated samples were centrifuged at 15,000 rpm for 15 min to remove any titanium particle shed from the microtip during sonication. Samples were kept overnight in dark at room temperature for equilibration before making measurements.

To prepare regenerated LUVs (RLUV) from SUVs, the samples were freeze-thawed five times using liquid nitrogen and then extruded through polycarbonate filters (pore diameter of 100 nm) mounted in the Avestin Liposofast Extruder as previously described. Samples were kept overnight in dark at room temperature for equilibration before making measurements. Background samples were prepared the same way except that the fluorophore was not added to them. All the measurements were performed at 23°C to ensure that DPPC is in the gel phase with the exception of the experiments described in Figs. 10 and 11 in which the measurements involving DPPC in the fluid phases were performed at 55°C.

All experiments in which the membrane thickness was changed were done using LUVs made from 640 nmol of a phospholipid (DLPC, DMPC, DPPC, DSPC, or DAPC) containing 0.1 to 2.0% (mol/mol) NBD-cholesterol prepared by the extrusion procedure as described above. The temperature of the buffer during swelling of the dried lipid mixtures was always maintained above the corresponding phase transition temperature of the specific lipid being used (Koynova and Caffrey, 1998) as the vesicles were made. The phospholipids used were of varying chain lengths: DLPC (12:0), DMPC (14:0), DPPC (16:0), DSPC (18:0), and DAPC (20:0). Samples were kept overnight in dark at room temperature for equilibration before making measurements.

Absorption measurements

The absorption spectra were obtained using a Hitachi U-2000 UV-visible absorption spectrophotometer (Hitachi, Ltd., Tokyo, Japan). Quartz cuvettes with a path length of 1 cm were used. Background samples without the fluorophore were used for baseline corrections.

Steady-state fluorescence measurements

Steady-state fluorescence measurements were performed with a Hitachi F-4010 spectrofluorometer using 1-cm path length quartz cuvettes. Excitation and emission slits with a nominal bandpass of 5 nm were used for all measurements. The excitation wavelength used was 484 nm in all cases. For recording excitation spectra, emission wavelength was kept fixed at 539 nm. Background intensities of samples in which NBD-cholesterol was omitted were subtracted from each sample spectrum to cancel out any contribution because of the solvent Raman peak and other scattering artifacts. All experiments were done with multiple sets of samples.

Time-resolved fluorescence measurements

Fluorescence lifetimes were calculated from time-resolved fluorescence intensity decays using a Photon Technology International (London, Ontario, Canada) LS-100 luminescence spectrophotometer in the time-correlated single photon counting mode. This machine uses a thyratron-gated nanosecond flash lamp filled with nitrogen as the plasma gas (16 ± 1 inches of mercury vacuum) and is run at 22–25 kHz. Lamp profiles were measured at the excitation wavelength using colloidal silica (Ludox; Dupont, Wilmington, DE) as the scatterer. To optimize the signal to noise ratio, 5000 photon counts were collected in the peak channel. The excitation wavelength used was 337 nm which corresponds to a peak in the spectral output of the nitrogen flash lamp. Emission wavelength was set at 522 or 539 nm. All experiments were performed using excitation and emission slits with a nominal bandpass of 4 nm or less. The sample and the scatterer were alternated after every 10% acquisition to ensure compensation for shape and timing drifts occurring during the period of data collection. The data stored in a multichannel analyzer was routinely transferred to an IBM PC for analysis. Intensity decay curves so obtained were fitted as a sum of exponential terms:

$$F(t) = \sum_i \alpha_i \exp(-t/\tau_i) \quad (1)$$

where α_i is a preexponential factor representing the fractional contribution to the time-resolved decay of the component with a lifetime τ_i. The decay parameters were recovered using a nonlinear least-squares iterative fitting procedure based on the Marquardt algorithm (Bevington, 1969). The program also includes statistical and plotting subroutine packages (O'Connor and Phillips, 1984). The goodness of the fit of a given set of observed data and the chosen function was evaluated by the reduced χ^2 ratio, the weighted residuals (Lampert et al., 1983), and the autocorrelation function of the weighted residuals (Grinvald and Steinberg, 1974). A fit was considered acceptable when plots of the weighted residuals and the autocorrelation function showed random deviation about zero with a minimum χ^2 value not more than 1.5. Mean (average) lifetimes $\langle\tau\rangle$ for biexponential decays of fluorescence were calculated from the decay times and preexponential factors using the following equation (Lakowicz, 1983):

$$\langle\tau\rangle = \frac{\alpha_1\tau_1^2 + \alpha_2\tau_2^2}{\alpha_1\tau_1 + \alpha_2\tau_2} \quad (2)$$

RESULTS

The fluorescence emission spectra of NBD-cholesterol in gel-phase DPPC vesicles of varying surface curvature are shown in Fig. 1. The concentration of NBD-cholesterol in these samples was kept constant at 2.0 mol %. We have previously shown that at this concentration, the transbilayer tail-to-tail dimers of NBD-cholesterol are formed in gel-phase DPPC vesicles and spectral features corresponding to the dimers predominate, i.e., emission maximum of fluorescence is found to be ~539 nm (Mukherjee and Chattopadhyay, 1996). Fig. 1 *A* shows that, in agreement with our previous results, the fluorescence emission maximum exhibited by NBD-cholesterol in gel-phase LUVs of DPPC is ~539 nm, which corresponds to the transbilayer cholesterol dimer. However, when the LUVs of DPPC were sonicated to produce SUVs which have more curvature stress (Huang and Mason, 1978) because of their small size (diameter ~250 Å), the fluorescence emission spectrum shows a distinct peak at ~522 nm which was absent in LUVs (Fig. 1 *B*). We have previously shown that at low concentrations (<0.5 mol %), the emission maximum of NBD-cholesterol in gel-phase DPPC vesicles is centered ~522 nm, which corresponds to the spectral feature of the NBD-cholesterol monomers in the membrane (Mukherjee and Chattopadhyay, 1996). This indicates that upon change of vesicle curvature, the monomer/dimer equilibrium of NBD-cholesterol in membranes is altered in such a way that in small, highly curved SUV, the monomer population is increased significantly (detected by the appearance of the 522-nm peak) even at a concentration (2.0 mol %) in which the NBD-cholesterol dimers predominate in large vesicles as shown earlier (Mukherjee and Chattopadhyay, 1996) and in Fig. 1 *a*. A similar result had earlier been reported using DHE as a probe (Loura and Prieto, 1997). To check the reversibility of the curvature effect on the monomer/dimer population (and to rule out any possible artifact from sonication), we regenerated large vesicles (termed as regenerated LUVs (RLUVs)) from SUVs by repeated freeze-thaw

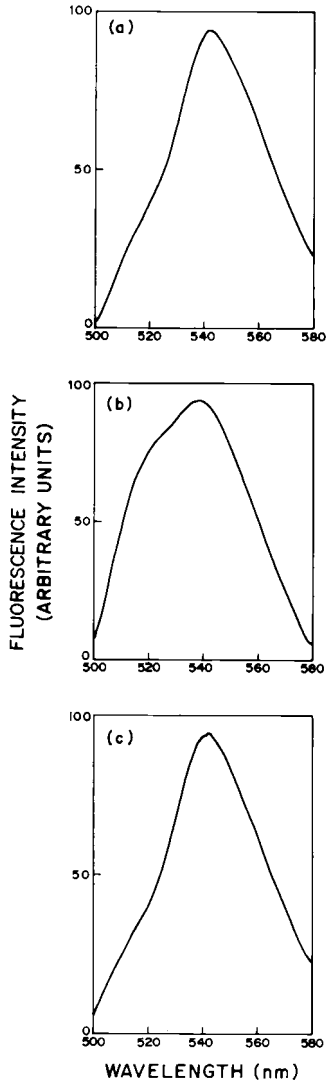

FIGURE 1 Fluorescence emission spectra of 2.0 mol % NBD-cholesterol in gel-phase DPPC vesicles of varying membrane surface curvature. The emission spectra correspond to LUVs (*a*), SUVs (*b*), and RLUVs (*c*) regenerated from SUVs of DPPC. The concentration of DPPC was 0.43 mM in all cases. The excitation wavelength was 484 nm. See Materials and Methods for other details.

followed by extrusion through polycarbonate filters of 100-nm pore diameter (see Materials and Methods) and monitored emission spectrum. Fig. 1 *c* shows that the monomer/dimer ratio is clearly dependent on the curvature of the membrane. Upon release of the curvature stress in RLUV, the spectral peak at 522 is lost and the emission spectrum shows a peak at ~539 nm which actually resembles the LUV spectrum shown in Fig. 1 *a*.

Fig. 2 shows that the reversible change in monomer/dimer ratio of NBD-cholesterol as a function of membrane curvature can also be monitored from the fluorescence excitation spectrum of NBD-cholesterol under these conditions. The concentration of NBD-cholesterol in these sam-

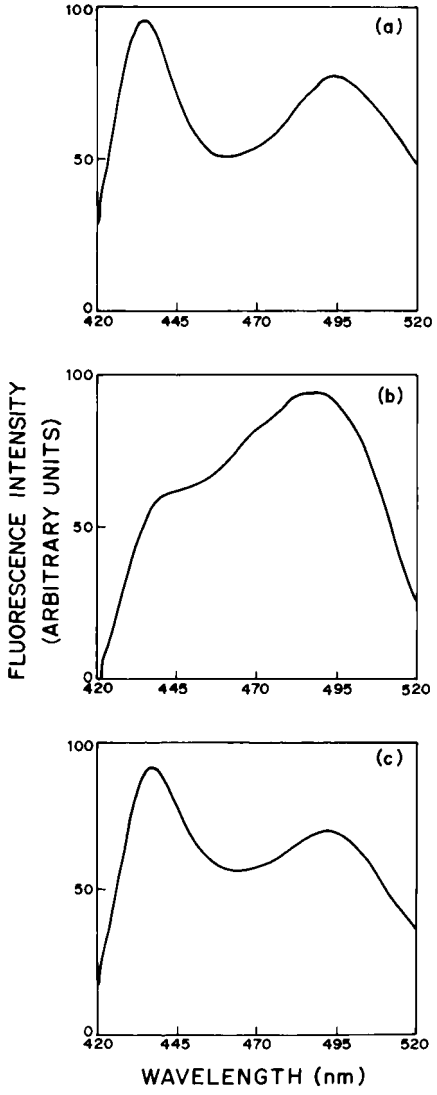

FIGURE 2 Fluorescence excitation spectra of 2.0 mol % NBD-cholesterol in gel-phase DPPC vesicles of varying membrane surface curvature. The excitation spectra correspond to LUVs (*a*), SUVs (*b*), and RLUVs (*c*) regenerated from SUVs of DPPC. The concentration of DPPC was 0.43 mM in all cases. The emission wavelength was kept fixed at 539 nm. See Materials and Methods for other details.

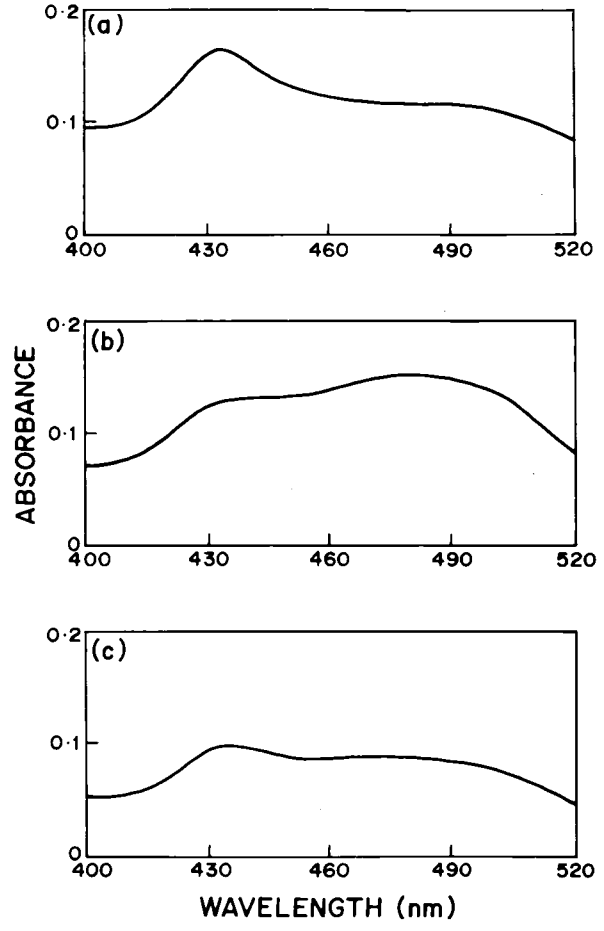

FIGURE 3 Absorption spectra of 2.0 mol % NBD-cholesterol in gel-phase DPPC vesicles of varying membrane surface curvature. The absorption spectra correspond to (*a*) LUVs, (*b*) SUVs, and (*c*) RLUVs regenerated from SUVs of DPPC. The concentration of DPPC was 0.43 mM in all cases. All other conditions are as in Fig. 1. See Materials and Methods for other details.

ples was also kept constant at 2.0 mol %. Fig. 2 *a* shows the characteristic structured fluorescence excitation spectrum of 2.0 mol % NBD-cholesterol in LUV of DPPC with two distinct peaks at ~436 and 494 nm. In agreement with our observation of curvature-dependent fluorescence emission spectrum (Fig. 1), the spectral features of the excitation spectrum change considerably in SUV. The 436 nm peak is reduced in intensity and merges with the peak at 494 nm which broadens and increases in intensity. We interpret the altered spectral features shown in Fig. 2 *b* attributable to an increase in NBD-cholesterol monomers. These spectral changes are reversed in this case also as shown in the excitation spectrum in RLUV which exhibits the characteristic spectrum with two distinct peaks at ~436 and 494 nm (Fig. 2 *c*) as observed in LUVs of DPPC in Fig. 2 *a*.

We have shown that the specific association of NBD-cholesterol in membranes at low concentrations is attributable to the formation of a ground-state complex and is not a result of an excited state interaction between NBD groups (Mukherjee and Chattopadhyay, 1996). Nevertheless, to demonstrate that the reversible change in NBD-cholesterol organization induced by change in membrane curvature is not based on any interaction in the excited state, we recorded absorption spectra under these conditions. Because the absorption process is instantaneous, and no physical displacement is allowed in this timescale, the information obtained from an absorption spectrum corresponds to the distribution of the fluorophores as they were in the ground state. The absorption spectrum of 2.0 mol % NBD-cholesterol in LUV of DPPC is shown in Fig. 3 *a*. As reported earlier (Mukherjee and Chattopadhyay, 1996), the absorp-

tion spectrum shows a distinct peak at ~436 nm in gel-phase DPPC which indicates the presence of NBD-cholesterol dimers. This peak was absent when the concentration of NBD-cholesterol was < 0.5 mol % (Mukherjee and Chattopadhyay, 1996). In agreement with the results obtained with fluorescence excitation and emission spectra, the absorption spectrum also gets altered when the membrane curvature is changed to produce SUVs. The absorption spectrum of 2.0 mol % NBD-cholesterol in SUV of DPPC is shown in Fig. 3 *B*, which shows that the peak at 436 nm, characteristic of the presence of NBD-cholesterol dimers, is considerably reduced. More interestingly, a new broad peak appears at 472 nm which is indicative of the increase in the population of monomers of NBD-cholesterol (Fig. 3 *B*). The spectral features change again when RLUV is formed when the new peak at 472 nm disappears and the original peak at 436 nm reappears, suggesting that the reversal of membrane curvature results in an enrichment of NBD-cholesterol dimers.

Because fluorescence lifetime serves as a sensitive indicator for the local environment in which a given fluorophore is placed, the change in organization experienced by the NBD moiety in the dimerization process could be reflected in its lifetime. To obtain the lifetimes of the two different populations of NBD-cholesterol that are centered at 522 and 539 nm (the predominantly monomer and dimer population, respectively) and to monitor their reversible interconversion with membrane curvature, fluorescence intensity decays were acquired under these conditions at both these wavelengths with the excitation wavelength at 337 nm. A typical intensity decay profile with its biexponential fitting and the various statistical parameters used to check the goodness of fit is shown in Fig. 4. Table 1 shows the fluorescence lifetimes of 2.0 mol % NBD-cholesterol in gel-phase DPPC vesicles of varying surface curvature. All fluorescence decays could be fitted well with a biexponential function. Table 1 shows that the mean lifetime, calculated using Eq. 2, of 2.0 mol % NBD-cholesterol in gel-phase LUV of DPPC is 7.22 ns when emission was monitored at 539 nm. At this concentration of NBD-cholesterol, the transbilayer tail-to-tail dimers of NBD-cholesterol are present in gel-phase DPPC vesicles; this value reflects a population in which the dimer form predominates. However, the mean lifetime is considerably shortened (~33%) to 4.84 ns when the membrane surface curvature is changed by generating SUVs of DPPC by sonication. The fluorescence lifetime of the NBD group is known to decrease in the presence of polar solvents such as water (Lin and Struve, 1991; Rawat and Chattopadhyay, 1999). The shortening of NBD lifetime in SUV could be attributable to increased water penetration in SUV because of high curvature stress which gives rise to packing defects (Yogev et al., 1991). Interestingly, when the membrane curvature is restored by producing RLUVs, the mean lifetime is increased to 6.77 ns which is very similar to the mean lifetime obtained with the original LUV of

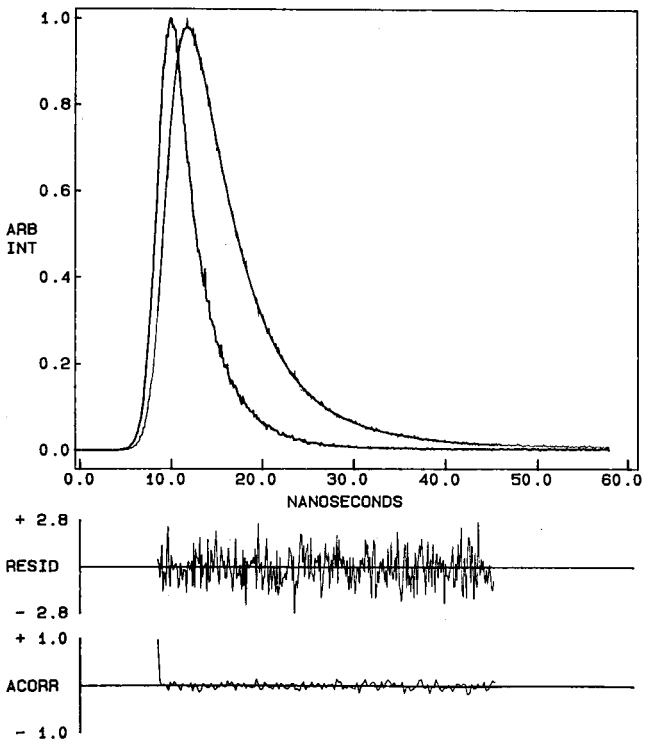

FIGURE 4 Time-resolved fluorescence intensity decay of 2.0 mol % NBD-cholesterol in LUVs of DPPC in the gel phase. Excitation was at 337 nm which corresponds to a peak in the spectral output of the nitrogen lamp. Emission was monitored at 522 nm. The sharp peak on the left is the lamp profile. The relatively broad peak on the right is the decay profile, fitted to a biexponential function. The two lower plots show the weighted residuals and the autocorrelation function of the weighted residuals. The concentration of DPPC was 0.85 mM. See Materials and Methods for other details.

DPPC (7.22 ns), thus indicating that the NBD-cholesterol dimers are reformed upon regenerating vesicles of low curvature.

The mean lifetimes obtained are somewhat more when observed at the longer emission wavelength (539 nm) compared with the values obtained using the shorter emission wavelength (522 nm). This is consistent with earlier observations (Lakowicz et al., 1983; Chattopadhyay and Mukherjee, 1993) in which such an increase in fluorescence lifetime

TABLE 1 Lifetimes of NBD-cholesterol in vesicles of varying membrane surface curvature at excitation wavelength 337 nm

Vesicle Type	α_1	τ_1 (ns)	α_2	τ_2 (ns)	$\langle\tau\rangle$ (ns)
LUV*	0.85	3.03	0.15	10.85	6.06
SUV	0.90	1.95	0.10	7.52	3.62
RLUV	0.84	2.60	0.16	9.25	5.29
LUV†	0.78	2.93	0.22	11.20	7.22
SUV	0.85	2.37	0.15	8.66	4.84
RLUV	0.76	3.01	0.24	10.27	6.77

*Emission wavelength 522 nm.
†Emission wavelength 539 nm.

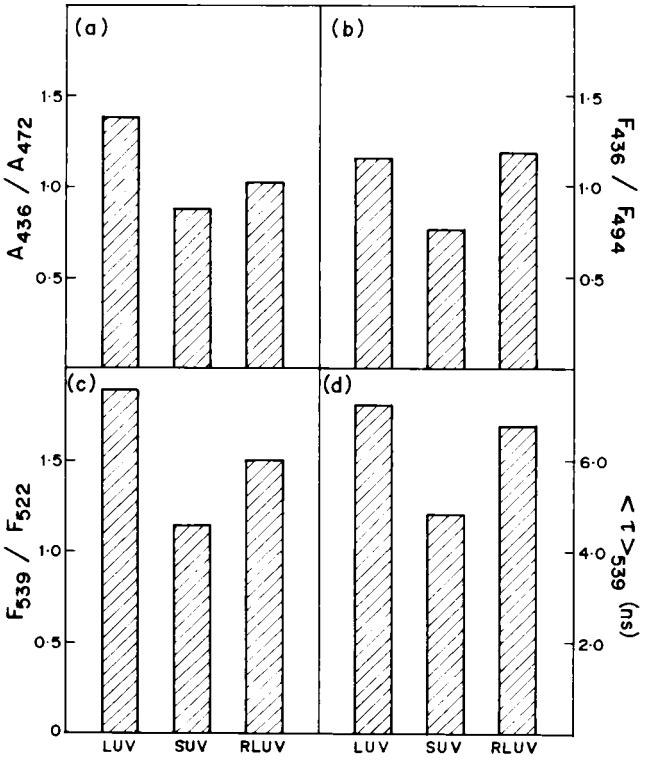

FIGURE 5 A comprehensive representation of spectral parameters showing the effect of curvature stress on cholesterol organization in membranes at low concentrations: change in absorbance ratio at 436 and 472 nm (*a*), ratio of fluorescence intensities at excitation wavelengths 436 and 494 nm (*b*), ratio of fluorescence intensities at emission wavelengths 539 and 522 nm (*c*), and mean fluorescence lifetimes $\langle\tau\rangle$ (calculated using Eq. 2) of 2.0 mol % NBD-cholesterol in gel-phase DPPC vesicles of varying membrane surface curvature (*d*).

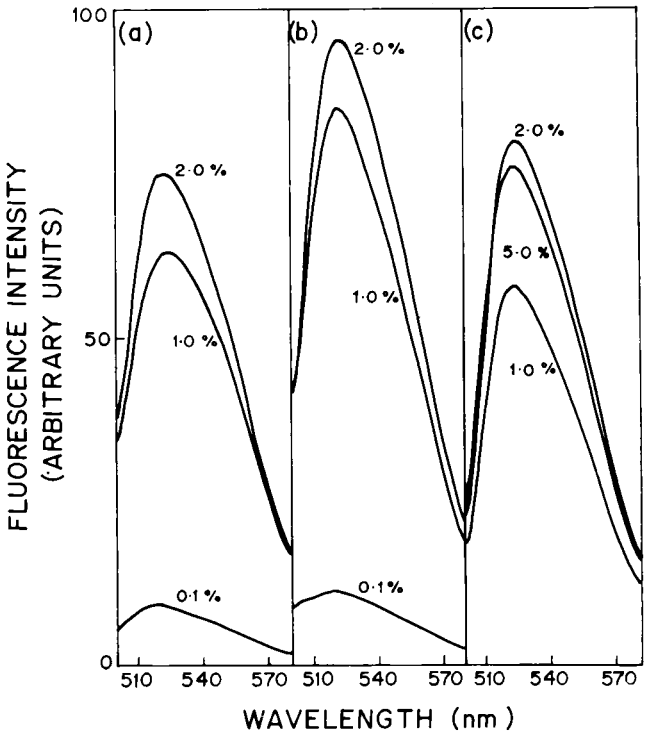

FIGURE 6 Fluorescence emission spectra of NBD-cholesterol in membranes of varying thickness. The emission spectra correspond to different concentrations of NBD-cholesterol in LUVs of gel-phase DAPC (*a*), gel-phase DSPC (*b*), and fluid-phase DLPC (*c*). The sample temperature was 23°C in all cases. The concentration of the specific phospholipid used was 0.43 mM in all cases, whereas the NBD-cholesterol concentrations in the samples were 0.43 μM (0.1 mol %), 4.3 μM (1.0 mol %), 8.6 μM (2.0 mol %), and 21.5 μM (5.0 mol %). The excitation wavelength was 484 nm in all cases. See Materials and Methods for other details.

with increasing emission wavelength (keeping the excitation wavelength constant) has been reported in motionally restricted media such as the membrane. Table 1 also shows that the reversal of mean lifetime accompanied with restoration of the original vesicle curvature is independent of the wavelength at which fluorescence emission is monitored because the mean fluorescence lifetime obtained using an emission wavelength of 522 nm shows a very similar trend in both cases.

These results using absorption and fluorescence (excitation and emission) spectral features with altered vesicle curvature point out that the organization of NBD-cholesterol in gel-phase DPPC membranes undergoes a change in terms of monomer/dimer population ratio in response to membrane surface curvature change even as the concentration is kept constant at 2.0 mol %. These results are reinforced by the corresponding changes in mean fluorescence lifetime. A comprehensive representation of all the spectral parameters showing the effect of curvature stress on cholesterol organization in membranes at low concentrations is shown in Fig. 5. It is clear from Fig. 5 that the organization of NBD-cholesterol in any type of membrane is dependent on its curvature and this conclusion is independent of the actual parameter used.

To examine the sensitivity of the transbilayer dimer organization to variations in membrane thickness, we monitored the fluorescence emission spectrum of NBD-cholesterol in membranes of varying acyl chain length. Fig. 6 *A* and *B* shows the emission spectra of NBD-cholesterol in different concentrations (0.1–2.0 mol %) in LUVs of DAPC and DSPC in the gel phase. DAPC and DSPC have 20 and 18 carbon atoms in their respective fatty acyl chains and the thickness of the lipid bilayers formed by them is more than bilayers of DPPC, which has 16 carbon atoms (Lewis and Engelman, 1983). The shape of the fluorescence emission spectra remains invariant in both cases at all concentrations and the emission maximum is centered at ~522 nm. In addition, the spectra are smooth and homogeneous even at 2.0 mol % NBD-cholesterol. This is in sharp contrast to what is observed with DPPC vesicles where a new peak at 539 nm appears at concentrations >0.1 mol % and the spectra become broad and inhomogeneous (Fig. 2, Mukherjee and Chattopadhyay, 1996), indicating the growing presence of NBD-cholesterol dimers with increase in concen-

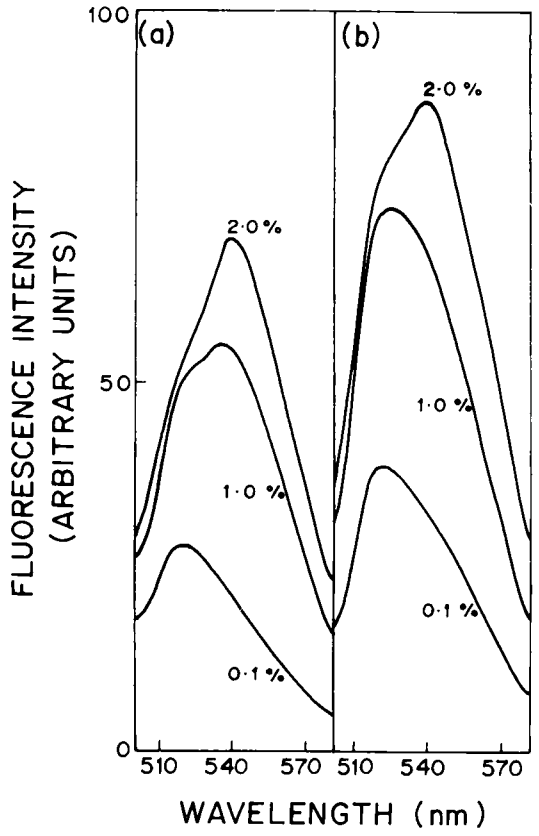

FIGURE 7 Fluorescence emission spectra of NBD-cholesterol in membranes of varying thickness. The emission spectra correspond to different concentrations of NBD-cholesterol in LUVs of (*a*) DPPC, (*b*) DMPC, both in the gel phase. The sample temperature was 23°C for DPPC vesicles whereas it was maintained at 15°C for DMPC vesicles. The concentration of DPPC or DMPC used was 0.43 mM in all cases, whereas the concentrations of NBD-cholesterol in the samples were 0.43 μM (0.1 mol %), 4.3 μM (1.0 mol %), and 8.6 μM (2.0 mol %). The excitation wavelength was 484 nm in all cases. See Materials and Methods for other details.

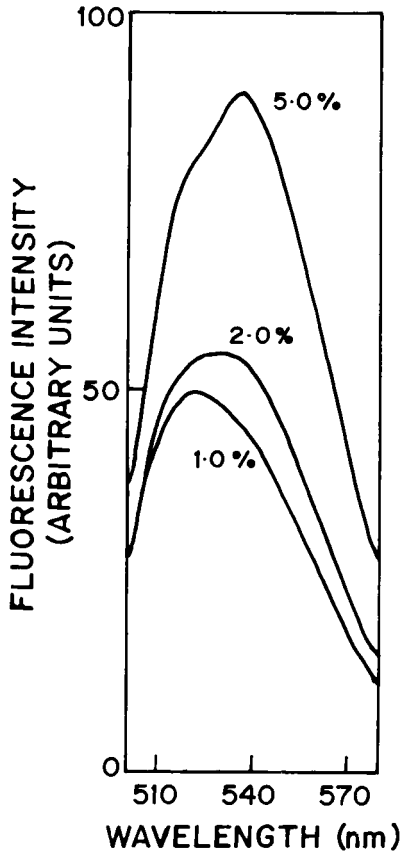

FIGURE 8 Fluorescence emission spectra of varying concentrations of NBD-cholesterol in LUVs of DPPC/sphingomyelin (70:30, mol/mol). The concentration of total lipid used was 0.43 mM, whereas the NBD-cholesterol concentrations in the samples were 4.3 μM (1.0 mol %), 8.6 μM (2.0 mol %), and 21.5 μM (5.0 mol %). The excitation wavelength was 484 nm. See Materials and Methods for other details.

tration. Therefore, we conclude that the dimers are not formed in gel-phase membranes made with longer chain lipids such as DAPC and DSPC where the membrane thickness is more, and that an optimal membrane thickness is required for the dimerization of NBD-cholesterol. This is further supported by experiments (Fig. 6 *c*) in which the fluorescence emission spectra of different concentrations (0.1–5.0 mol %) of NBD-cholesterol is monitored in LUVs of DLPC (containing 12 carbon atoms in its acyl chain) in the fluid phase. As shown in Fig. 6 *c*, the maximum of fluorescence emission remains centered at ~522 nm at all concentrations and the spectra are smooth and homogeneous even at 5.0 mol % NBD-cholesterol. This shows that the NBD-cholesterol dimers are not detected in the relatively thin DLPC membranes. In contrast to this, Fig. 7 shows the emission spectra of varying concentrations of NBD-cholesterol in DPPC and DMPC membranes in the gel phase. The spectrum is smooth and homogeneous when NBD-cholesterol concentration is kept extremely low (0.1 mol %) with the maximum of fluorescence emission at ~522 nm. As the NBD-cholesterol concentration increases, the spectra start showing deviations and a new peak centered at ~539 nm seems similar to our earlier report (Mukherjee and Chattopadhyay, 1996). The spectra also become broad and inhomogeneous at higher concentrations. Taken together, these results show that the dimers of NBD-cholesterol are formed in DPPC and DMPC membranes in the gel phase but not in thicker DSPC and DAPC membranes. The process of dimerization is therefore well regulated by membrane thickness.

Sphingomyelins have been implicated in many cases in the formation of lipid microdomains, especially in the presence of cholesterol (Brown, 1998). To assess whether such dimerization of NBD-cholesterol takes place in membranes containing sphingomyelin, we monitored the fluorescence emission spectrum of varying concentrations (1–5 mol %) of NBD-cholesterol in LUVs of DPPC containing 30 mol % of sphingomyelin. These results are depicted in Fig. 8, which shows that the maximum of fluorescence emission

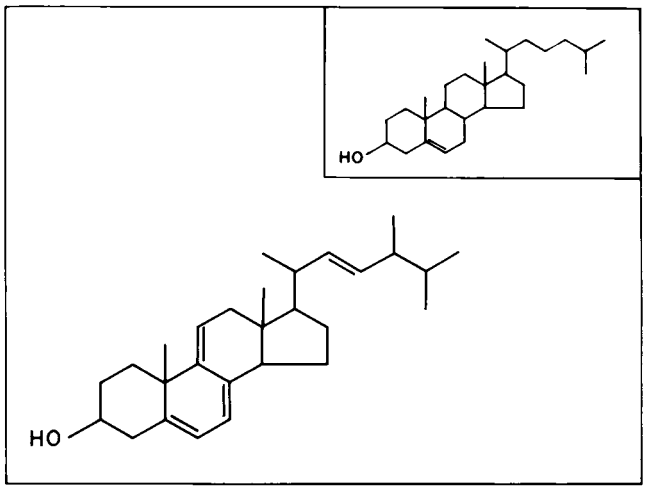

FIGURE 9 Chemical structure of DHE. The structure of cholesterol is shown in the inset for comparison.

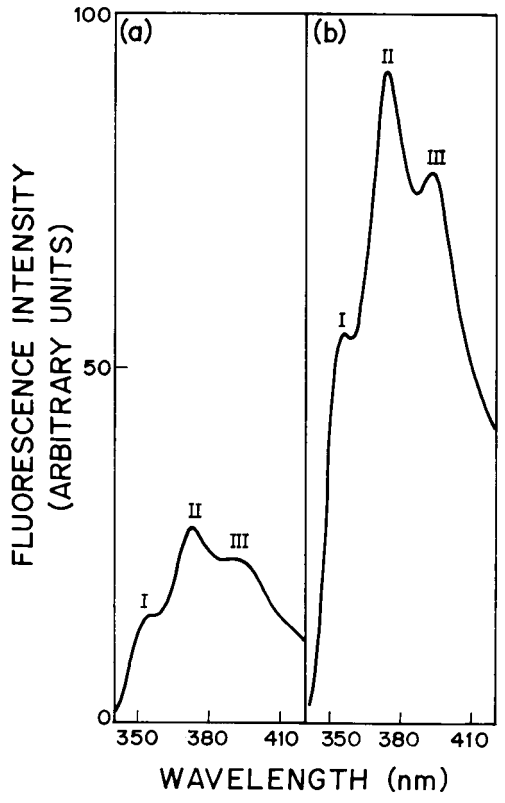

FIGURE 10 Fluorescence emission spectra of 2.0 mol % DHE in LUVs of DPPC in fluid phase (*a*) and in gel phase (*b*). The sample temperature was maintained at 55°C for the fluid-phase experiment whereas the gel-phase experiment was performed at 23°C. The emission maxima at 355, 374, and 394 nm are marked as I, II, and III, respectively. The concentration of DPPC was 0.43 mM in both cases. The excitation wavelength was 324 nm. See Materials and Methods for other details.

spectrum is centered at ~522 nm when the concentration of NBD-cholesterol is 1 mol %. However, the emission spectra at NBD-cholesterol concentrations >1 mol % display a shift in emission maximum with an emission maximum of 539 nm at 5 mol %, similar to what is observed with DPPC vesicles alone. This shows that the process of dimerization also takes place in sphingomyelin-containing membranes.

If the local organization exhibited by cholesterol in membranes of low cholesterol content is a general phenomenon, it should not be dependent on the probe chosen. To examine this issue, we performed experiments in which we monitored an environment-sensitive spectral feature (peak intensity ratio) of DHE as a function of concentration. DHE is a naturally occurring fluorescent cholesterol analog which is found in yeast and differs from cholesterol in having three additional double bonds and a methyl group (Fig. 9). A number of studies have shown that DHE faithfully mimics natural cholesterol in biophysical, biochemical, and cell biological studies (Schroeder et al., 1991, 1995).

The fluorescence emission spectra of DHE in DPPC vesicles in fluid and gel phase are shown in Fig. 10. A characteristic feature of the structured emission spectra are the maxima at 355, 374, and 394 nm, denoted as I, II, and III, respectively. This type of structured vibronic band intensities are known to be sensitive to environment. This has been effectively used for elucidating microenvironments of the hydrophobic fluorophore pyrene whose emission spectrum shows similar vibronic fine structure (Kalyansundaram and Thomas, 1977). In particular, the ratio of emission maxima was shown to be sensitive to aggregation state of the fluorophore and environmental polarity (Kalyansundaram and Thomas, 1977). We used this sensitive spectral feature of DHE to monitor its change in local organization at low concentrations in membranes. Fig. 11 shows the change in peak intensity ratios (F_{394}/F_{355} and F_{374}/F_{355}) as a function of DHE concentration in LUV of gel and fluid phase DPPC (Fig. 11, *a* and *b*) and in fluid phase DLPC, and gel-phase DSPC (Fig. 11, *c* and *d*, respectively). The fluorescence intensity ratio initially increases with increasing DHE concentration in all cases and then attains a steady value. We attribute this change in slope to the change in local organization of DHE. Fig. 11 shows that for gel-phase DPPC membranes (*a*), the intensity ratio changes sharply and assumes a steady value at DHE concentrations ≥1.0 mol %. In contrast, in case of fluid-phase DPPC, fluid-phase DLPC, or gel-phase DSPC vesicles, the change in slope is much more gradual and is observed at a much higher concentration. The intensity ratio does not seem to assume a constant value even at higher concentrations in these cases. This indicates that the change in local organization of DHE occurs at a low concentration in gel-phase DPPC vesicles but not in the other cases. This is in excellent agreement with Fig. 6 and with our earlier observation using NBD-cholesterol (Figs. 10 and 11, Mukherjee and Chattopadhyay, 1996) where the appearance of a new fluorescence or absorbance peak was observed at NBD-cholesterol ≥1.0

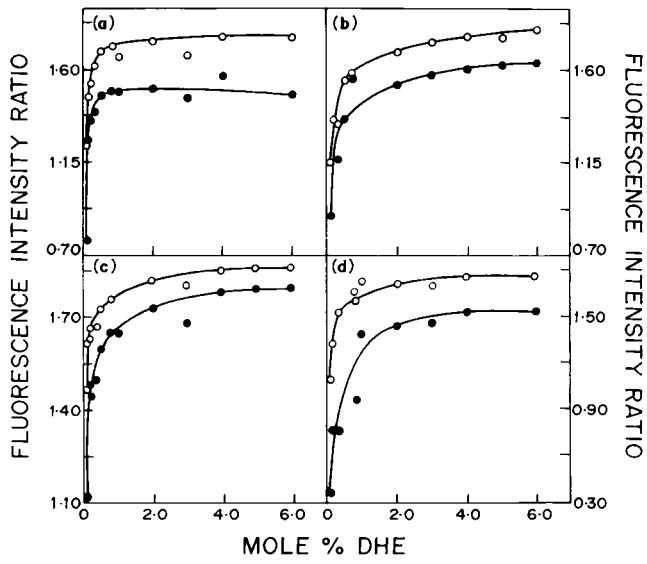

FIGURE 11 Change in peak intensity ratios F_{394}/F_{355} (●) and F_{374}/F_{355} (○) as a function of DHE concentration in LUVs of gel-phase DPPC (*a*), fluid-phase DPPC (*b*), fluid-phase DLPC (*c*), and gel-phase DSPC (*d*). The sample temperature was maintained at 23°C in all cases except in the case of gel-phase DPPC (*b*) in which a temperature of 55°C was maintained. The concentration of the phospholipid was 0.43 mM in all cases. The excitation wavelength was 324 nm. See Materials and Methods for other details.

mol % in the gel phase and at a much higher concentration (≥5.0 mol %) in the fluid phase.

DISCUSSION

Very little is known about the organization and dynamics of membranes when the cholesterol content is very low (<5.0 mol %). Because there are a number of intracellular organelles such as the ER and the inner mitochondrial membrane where the cholesterol content is actively maintained at a low level (Bretscher amd Munro, 1993; Lange, 1991), any information on cholesterol organization in such membranes will be useful. It has recently been reported (Lemmich et al., 1997) that low amounts (<3.0 mol %) of cholesterol contribute to softness of the membrane. Cholesterol in amounts up to 3.0 mol % softens the lipid bilayer and only at concentrations higher than 4.0 mol % leads to the well known effect of rigidification, which is responsible for the mechanical coherence of eukaryotic plasma membranes. In another study (Raffy and Teissié, 1999), membrane permeability changes at very low cholesterol concentrations have been studied and were very different from results obtained at high concentrations of cholesterol.

We have previously shown that cholesterol may exhibit local organization even at very low concentrations (<2.0 mol %) in membranes using NBD-cholesterol. Our results indicated the possible presence of transbilayer tail-to-tail dimers of cholesterol in such membranes (Mukherjee and Chattopadhyay, 1996). This is supported by similar observations reported by other groups obtained under comparable cholesterol concentrations (Harris et al., 1995; Loura and Prieto, 1997). We show that some of the basic features of cholesterol organization in membranes at low concentrations obtained using NBD-cholesterol are in agreement with concentration-dependent changes observed in certain spectral features of DHE, a naturally occurring fluorescent cholesterol analog which closely mimics cholesterol.

The overall goal of this paper is to examine the role of membrane surface curvature and thickness on transbilayer dimerization occurring at low cholesterol concentrations using NBD-cholesterol as a fluorescent cholesterol analog. Our results show that the transbilayer dimer arrangement of cholesterol, observed previously (Mukherjee and Chattopadhyay, 1996; Harris et al., 1995; Loura and Prieto, 1997), is sensitive to surface curvature of the membrane and cholesterol dimerization is not favored in highly curved membranes. Thus, the monomer/dimer equilibrium is shifted toward monomers upon sonication of DPPC LUVs, i.e., by increasing surface curvature in SUVs. Characteristic features of SUVs include small size and higher (~ 60–70% of total) population of lipids in the outer leaflet (Huang and Mason, 1978). The average area per lipid headgroup and effective length of the lipid are greater in the outer leaflet than in the inner leaflet of SUVs, which gives rise to dynamic transmembrane asymmetry. The packing of lipid molecules are thus quite different in the two leaflets of SUVs (the inner leaflet being more constrained) and this mismatch in packing in the two monolayers could inhibit the transbilayer tail-to-tail interaction necessary for the dimer formation. The equilibrium is shifted back toward dimers upon release of the curvature stress by RLUVs, as evidenced by the reversible modulation of the spectral features we monitored. In addition, we have investigated the effect of bilayer thickness on the monomer/dimer equilibrium of NBD-cholesterol. Our results show that the dimers of NBD-cholesterol are formed in DPPC and DMPC membranes in the gel phase but not in thicker DSPC and DAPC membranes. Interestingly, NBD-cholesterol dimers are not detected in the relatively thin DLPC membranes either. We therefore conclude that the process of dimerization is stringently controlled by a narrow window of membrane thickness. A comprehensive representation of these two effects (effects of curvature stress and membrane thickness on the organization of NBD-cholesterol in membranes at low concentrations) is schematically shown in Fig. 12.

The nature of the putative dimer organization of NBD-cholesterol deserves comment. It has been previously shown that the NBD group in NBD-cholesterol is located close to the center of the bilayer (Chattopadhyay and London, 1987). This spatial arrangement would bring the NBD groups from opposite leaflets in close proximity and make the interaction of the two NBD groups energetically favorable. [This would not be true, for example, if the NBD

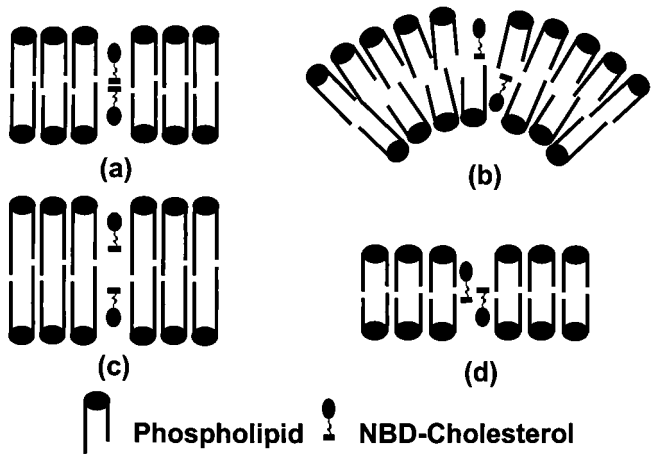

FIGURE 12 A schematic diagram of the membrane bilayer showing the effects of curvature stress and membrane thickness on the organization of NBD-cholesterol in membranes at low concentrations. (*a*) The transbilayer tail-to-tail dimers of NBD-cholesterol proposed earlier (Mukherjee and Chattopadhyay, 1996). (*b*) NBD-cholesterol monomers in membranes with high surface curvature such as SUVs. (*c*) NBD-cholesterol monomers in relatively thick membranes formed by phospholipids having longer fatty acyl chains. (*d*) NBD-cholesterol monomers in relatively thin membranes formed by phospholipids having shorter fatty acyl chains. See text for other details.

group looped up in the bilayer as is often seen with NBD-labeled phospholipids with NBD groups placed at the end of the fatty acyl chain (Chattopadhyay and London, 1988).] Fluorophores, when placed close to each other without any specific pattern (spatial arrangement) of organization, often give rise to self-quenching (Chattopadhyay et al., 1992). In fact, concentration-dependent self-quenching of the NBD group is well characterized and constitutes the basis of a number of assays in membrane biology because this type of quenching is very sensitive to local surface density of lipids in the membrane (Nichols and Pagano, 1981; Chattopadhyay, 1990). It is interesting that the association of the NBD groups from the opposing leaflets in this case does not give rise to self-quenching, but, instead, gives rise to a new peak and other well defined spectral features in the fluorescence and absorption spectra (Figs. 1–3). The unique spectral features imply that the two NBD groups are not only close in space but have a definite spatial orientation which would have been lacking otherwise. That this is a ground-state phenomenon is supported by the concomitant changes in absorption spectrum with changes in fluorescence spectra. An important factor contributing to the stability of the NBD-cholesterol dimers is aromatic-aromatic interaction between the NBD rings. However, the possibility of other types of association cannot be ruled out from the present data. Moreover, at this point it is not clear whether the dimers can lead to further aggregation. The formation of such transmembrane dimers could represent the first step in the ultimate separation of a pure cholesterol domain.

The transbilayer tail-to-tail cholesterol organization could have a role in diseased states. The importance of cholesterol transbilayer domains in atherogenesis was recently demonstrated by Tulenko et al. (1998). In this study, small angle x-ray diffraction was used to examine arterial smooth muscle cell plasma membranes isolated from control and cholesterol-fed (2.0%) atherosclerotic rabbits. Beyond 9 weeks of cholesterol feeding, x-ray diffraction patterns demonstrated a lateral immiscible cholesterol domain with a bilayer thickness of 34 Å coexisting with the liquid crystalline (fluid) lipid bilayer. The membrane thickness of 34 Å corresponds to a tail-to-tail arrangement of cholesterol dimers as the length of an individual cholesterol molecule is 17 Å (Craven, 1976). This points out the possible involvement of the transbilayer tail-to-tail organization of cholesterol in atherogenesis.

Such cholesterol domains found in membranes of low cholesterol content (such as the ER or the inner mitochondrial membrane) could have important functional implications in intracellular sorting and trafficking. The low cholesterol content of the ER membrane has been attributed to its need to be readily deformable in order for newly synthesized membrane proteins to be folded and assembled properly (Bretscher and Munro, 1993). It has been suggested that the specific gradient of cholesterol concentration found in Golgi and ER facilitates protein sorting in the secretory pathway via cholesterol's ability to modify the membrane thickness (Pelham and Munro, 1993). Membrane softening caused by low levels of cholesterol (Lemmich et al., 1997) may play a role in the vesicle budding process associated with membrane traffic in Golgi and ER. Cholesterol is removed from ER, its site of synthesis, by using the membrane traffic pathway where membranes move from the ER to the plasma membrane through the Golgi apparatus. Cholesterol is known to modulate lipid-protein interactions by increasing the thickness of the lipid bilayer. For example, it has been shown that 1-palmitoyl-2-oleoyl-*sn*-glycero-3-phosphocholine vesicles have a bilayer thickness of ~26 Å which increases to 30 Å in the presence of 30 mol % cholesterol (Nezil and Bloom, 1992). In fact, there is evidence that a gradient of cholesterol exists in Golgi and the membrane coming from the Golgi apparatus is believed to be thicker and to have more cholesterol than the membrane entering from the ER. Because our results show that cholesterol dimerization is controlled by membrane thickness, this could imply that there is a gradient of cholesterol dimers across the Golgi apparatus.

It is noteworthy that many important cellular trafficking events (such as vesiculation, tubulation, pinching off of endocytic vesicles, and fusion of exocytic vesicles) are accompanied by sharp changes in membrane curvature (Zimmerberg, 2000). The overall process of membrane trafficking and turnover is influenced by membrane curvature, e.g., vesicles budding from ER or Golgi may have more surface curvature than their parent membrane. Curvature-

induced membrane domains have recently been reported to be responsible for differential sorting and trafficking of lipid analogs in CHO cells (Mukherjee et al., 1999). Some of the vesicles involved in cellular traffic, e.g., coated vesicles used in exocytosis, are quite small (~500 Å diameter, comparable with SUV dimensions) and are highly curved (Aridor and Balch, 1996). Certain regions of sorting endosomes experience high curvature stress (Mukherjee et al., 1999). The endosomal vesicles also experience low (acidic) pH (Mukherjee et al., 1997). Interestingly, it has recently been reported that pH has a strong effect on the membrane curvature (Lee et al., 1999).

In summary, we have investigated the role of membrane surface curvature and thickness on transbilayer dimerization occurring at low concentrations of cholesterol using NBD-cholesterol as a fluorescent cholesterol analog. Our results show that the transbilayer dimer arrangement of cholesterol previously observed at low concentrations in membranes is sensitive to the membrane surface curvature and is stringently controlled by a narrow window of membrane thickness. These results are significant in the context of cholesterol organization in membranes at low concentrations in particular, and in the dynamics and regulation of cellular cholesterol, in general.

We thank Y. S. S. V. Prasad and G. G. Kingi for technical help. This work was supported by the Council of Scientific and Industrial Research, Government of India. S.S.R. thanks the Council of Scientific and Industrial Research for the award of a Senior Research Fellowship. S.C.B. thanks the Department of Biotechnology, Government of India, for the award of a postdoctoral fellowship. We thank Dr. K. G. Harikumar for critically reading the manuscript.

REFERENCES

Aridor, M., and W. E. Balch. 1996. Principles of selective transport: coat complexes hold the key. *Trends Cell Biol.* 6:315–320.

Bevington, P. R. 1969. Data Reduction and Error Analysis for the Physical Sciences. McGraw-Hill, New York.

Bretscher, M. S., and S. Munro. 1993. Cholesterol and the Golgi apparatus. *Science.* 61:1280–1281.

Brown, R. E. 1998. Sphingolipid organization in biomembranes: what physical studies of model membranes reveal. *J. Cell Sci.* 111:1–9.

Chattopadhyay, A. 1990. Chemistry and biology of *N*-(7-nitrobenz-2-oxa-1, 3-diazol-4-yl)-labeled lipids: fluorescent probes of biological and model membranes. *Chem. Phys. Lipids.* 53:1–15.

Chattopadhyay, A., and E. London. 1987. Parallax method for direct measurement of membrane penetration depth utilizing fluorescence quenching by spin-labeled phospholipids. *Biochemistry.* 26:39–45.

Chattopadhyay, A., and E. London. 1988. Spectroscopic and ionization properties of *N*-(7-nitrobenz-2-oxa-1, 3-diazol-4-yl)-labeled lipids in model membranes. *Biochim. Biophys. Acta.* 938:24–34.

Chattopadhyay, A., and S. Mukherjee. 1993. Fluorophore environments in membrane-bound probes: a red edge excitation shift study. *Biochemistry.* 32:3804–3811.

Chattopadhyay, A., and S. Mukherjee. 1999. Red edge excitation shift of a deeply embedded membrane probe: implications in water penetration in the bilayer. *J. Phys. Chem. B.* 103:8180–8185.

Chattopadhyay, A., S. S. Komath, and B. Raman. 1992. Aggregation of lasalocid A in membranes: a fluorescence study. *Biochim. Biophys. Acta.* 1104:147–150.

Craven, B. M. 1976. Crystal structure of cholesterol monohydrate. *Nature.* 260:727–729.

Dittmer, J. C., and R. L. Lester. 1964. A simple, specific spray for the detection of phospholipids on thin-layer chromatograms. *J. Lipid Res.* 5:126–127.

Fielding, C. J., and P. E. Fielding. 1997. Intracellular cholesterol transport. *J. Lipid Res.* 38:1503–1520.

Fery-Forgues, S., J.-P. Fayet, and A. Lopez. 1993. Drastic changes in the fluorescence properties of NBD probes with the polarity of the medium: involvement of a TICT state? *J. Photochem. Photobiol. A.* 70:229–243.

Gimpl, G., K. Burger, and F. Fahrenholz. 1997. Cholesterol as modulator of receptor function. *Biochemistry.* 36:10959–10974.

Grechishnikova, IV, F. Bergstrom, L. B.-A. Johansson, R. E. Brown, and J. G. Molotkovsky. 1999. New fluorescent cholesterol analogs as membrane probes. *Biochim. Biophys. Acta.* 1420:189–202.

Grinvald, A., and I. Z. Steinberg. 1974. On the analysis of fluorescence decay kinetics by the method of least-squares. *Anal. Biochem.* 59: 583–598.

Harris, J. S., D. E. Epps, S. R. Davio, and F. J. Kezdy. 1995. Evidence for transbilayer, tail-to-tail cholesterol dimers in dipalmitoylglycerophosphocholine liposomes. *Biochemistry.* 34:3851–3857.

Huang, C., and J. T. Mason. 1978. Geometric packing constraints in egg phosphatidylcholine vesicles. *Proc. Natl. Acad. Sci. U.S.A.* 75:308–310.

Incardona, J. P., and S. Eaton. 2000. Cholesterol in signal transduction. *Curr. Opin. Cell Biol.* 12:193–203.

Kalyansundaram, K., and J. K. Thomas. 1977. Environmental effects on vibronic band intensities in pyrene monomer fluorescence and their application in studies of micellar systems. *J. Am. Chem. Soc.* 99: 2039–2044.

Kobayashi, T., and R. E. Pagano. 1988. ATP-dependent fusion of liposomes with the Golgi apparatus of perforated cells. *Cell.* 55:797–805.

Koval, M., and R. E. Pagano. 1990. Sorting of an internalized plasma membrane lipid between recycling and degradative pathways in normal and Niemann-Pick, type A fibroblasts. *J. Cell. Biol.* 111:429–442.

Koynova, R., and M. Caffrey. 1998. Phases and phase transitions of the phosphatidylcholines. *Biochim. Biophys. Acta.* 1376:91–145.

Lakowicz, J. R. 1983. Principles of Fluorescence Spectroscopy. Plenum Press, New York.

Lakowicz, J. R., D. R. Bevan, B. P. Maliwal, H. Cherek, and A. Balter. 1983. Synthesis and characterization of a fluorescent probe of the phase transition and dynamic properties of membranes. *Biochemistry.* 22: 5714–5722.

Lampert, R. A., L. A. Chewter, D. Phillips, D. V. O'Connor, A. J. Roberts, and S. R. Meech. 1983. Standards for nanosecond fluorescence decay time measurements. *Anal. Chem.* 55:68–73.

Lange, Y. 1991. Disposition of intracellular cholesterol in human fibroblasts. *J. Lipid Res.* 33:329–339.

Lange, Y., M. H. Swaisgood, B. V. Ramos, and T. L. Stack. 1989. Plasma membranes contain half the phospholipid and 90% of the cholesterol and sphingomyelin in cultured human fibroblasts. *J. Biol. Chem.* 264: 3786–3793.

Lange, Y., J. Ye, M. Rigney, and T. L. Stack. 1999. Regulation of ER cholesterol by plasma membrane cholesterol. *J. Lipid Res.* 40: 2264–2270.

Lee, J. B., P. G. Petrov, and H.-G. Döbereiner. 1999. Curvature of zwitterionic membranes in transverse pH gradients. *Langmuir.* 15: 8543–8546.

Lemmich, J., K. Mortensen, J. H. Ipsen, T. Hønger, R. Bauer, and O. G. Mouritsen. 1997. The effect of cholesterol in small amounts on lipid-bilayer softness in the region of the main phase transition. *Eur. Biophys. J.* 25:293–304.

Lewis, B. A., and D. M. Engelman. 1983. Lipid bilayer thickness varies linearly with acyl chain length in fluid phosphatidylcholine vesicles. *J. Mol. Biol.* 166:211–217.

Liao, S., J. Lin, H. Do, and A. E. Johnson. 1997. Both lumenal and cytosolic gating of the aqueous ER translocon pore are regulated from inside the ribosome during membrane protein integration. *Cell.* 90: 31–41.

Lin, S., and W. S. Struve. 1991. Time-resolved fluorescence of nitrobenzoxadiazole-aminohexanoic acid: effect of intermolecular hydrogen-bonding on non-radiative decay. *Photochem. Photobiol.* 54:361–365.

Liscum, L., and K. W. Underwood. 1995. Intracellular cholesterol transport and compartmentalization. *J. Biol. Chem.* 270:15443–15446.

Liscum, L., and N. J. Munn. 1999. Intracellular cholesterol transport. *Biochim. Biophys. Acta.* 1438:19–37.

Loura, L. M. S., and M. Prieto. 1997. Dehydroergosterol structural organization in aqueous medium and in a model system of membranes. *Biophys. J.* 72:2226–2236.

Maccarrone, M., L. Bellincampi, G. Melino, and A. Finazzi Agro. 1998. Cholesterol, but not its esters, triggers programmed cell death in human erythroleukemia K562 cells. *Eur. J. Biochem.* 263:107–113.

MacDonald, R. C., R. I. MacDonald, B. P. Menco, K. Takeshita, N. K. Subbarao, and L. R. Hu. 1991. Small-volume extrusion apparatus for preparation of large, unilamellar vesicles. *Biochim. Biophys. Acta.* 1061: 297–303.

Mazeres, S., V. Schram, J.-F. Tocanne, and A. Lopez. 1996. 7-Nitrobenz-2-oxa-1,3-diazole-4-yl-labeled phospholipids in lipid membranes: differences in fluorescence behavior. *Biophys. J.* 71:327–335.

McClare, C. W. F. 1971. An accurate and convenient organic phosphorus assay. *Anal. Biochem.* 39:527–530.

McMullen, T. P. W., and R. N. McElhaney. 1996. Physical studies of cholesterol-phospholipid interactions. *Curr. Opin. Colloid Interface Sci.* 1:83–90.

Mitra, B., and G. G. Hammes. 1990. Membrane-protein structural mapping of chloroplast coupling factor in asolectin vesicles. *Biochemistry.* 29: 9879–9884.

Mukherjee, S., and A. Chattopadhyay. 1996. Membrane organization at low cholesterol concentrations: a study using 7-nitrobenz-2-oxa-1,3-diazol-4-yl-labeled cholesterol. *Biochemistry.* 35:1311–1322.

Mukherjee, S., A. Chattopadhyay, A. Samanta, and T. Soujanya. 1994. Dipole moment change of NBD group upon excitation using solvatochromic and quantum chemical approaches: implications in membrane research. *J. Phys. Chem.* 98:2809–2812.

Mukherjee, S., R. N. Ghosh, and F. R. Maxfield. 1997. Endocytosis. *Physiol. Rev.* 77:759–803.

Mukherjee, S., and F. R. Maxfield. 1999. Cholesterol: stuck in traffic. *Nature Cell Biol.* 1:E37–E38.

Mukherjee, S., Soe, T. T., and F. R. Maxfield. 1999. Endocytic sorting of lipid analogs differing solely in the chemistry of their hydrophobic tails. *J. Cell Biol.* 144:1271–1284.

Nezil, F. A., and M. Bloom. 1992. Combined influence of cholesterol and synthetic amphiphilic peptides upon bilayer thickness in model membranes. *Biophys. J.* 61:1176–1183.

Nichols, J. W., and R. E. Pagano. 1981. Kinetics of soluble lipid monomer diffusion between vesicles. *Biochemistry.* 20:2783–2789.

O'Connor, D. V., and D. Phillips. 1984. Time-Correlated Single Photon Counting. Academic Press, London. 180–189.

Pelham, H. R. B., and S. Munro. 1993. Sorting of membrane proteins in the secretory pathway. *Cell.* 75:603–605.

Porter, J. A., K. E. Young, and P. A. Beachy. 1996. Cholesterol modification of hedgehog signalling proteins in animal development. *Science.* 274:255–259.

Raffy, S., and J. Teissié. 1999. Control of lipid membrane stability by cholesterol content. *Biophys. J.* 76:2072–2080.

Rawat, S. S., and A. Chattopadhyay. 1999. Structural transition in the micellar assembly: a fluorescence study. *J. Fluorescence.* 9:233–244.

Schroeder, F. 1984. Fluorescent sterols: probe molecules of membrane structure and function. *Prog. Lipid Res.* 23:97–113.

Schroeder, F., A. A. Frolov, E. J. Murphy, B. P. Atshaves, J. R. Jefferson, L. Pu, W. G. Wood, W. B. Foxworth, and A. B. Kier. 1996. Recent advances in membrane cholesterol domain dynamics and intracellular cholesterol trafficking. *Proc. Soc. Exp. Biol. Med.* 213:150–177.

Schroeder, F., J. R. Jefferson, A. B. Kier, J. Knittel, T. J. Scallen, W. G. Wood, and I. Hapala. 1991. Membrane cholesterol dynamics: cholesterol domains and kinetic pools. *Proc. Soc. Exp. Biol. Med.* 196: 235–252.

Schroeder, F., J. K. Woodford, J. Kavecansky, W. G. Wood, and C. Joiner. 1995. Cholesterol domains in biological membranes. *Mol. Membr. Biol.* 12:113–119.

Simons, K., and E. Ikonen. 1997. Functional rafts in cell membranes. *Nature.* 387:569–572.

Simons, K., and E. Ikonen. 2000. How cells handle cholesterol. *Science.* 290:1721–1726.

Smutzer, G., B. F. Crawford, and P. L. Yeagle. 1986. Physical properties of the fluorescent sterol probe dehydroergosterol. *Biochim. Biophys. Acta.* 862:361–371.

Sparrow, C. P., S. Patel, J. Baffic, Y.-S. Chao, M. Hernandez, M.-H. Lam, J. Montenegro, S. D. Wright, and P. A. Detmers. 1999. A fluorescent cholesterol analog traces cholesterol absorption in hamsters and is esterified in vivo and in vitro. *J. Lipid Res.* 40:1747–1757.

Tulenko, T. N., M. Chen, P. E. Mason, and R. P. Mason. 1998. Physical effects of cholesterol on arterial smooth muscle membranes: evidence of immiscible cholesterol domains and alterations in bilayer width during atherogenesis. *J. Lipid Res.* 39:947–956.

Van Meer, G., E. H. Stelzer, R. W. Wijnaendts-van-Resandt, and K. Simons. 1987. Sorting of sphingolipids in epithelial (Madin-Darby canine kidney) cells. *J. Cell. Biol.* 105:1623–1635.

Xu, X., and E. London. 2000. The effect of sterol structure on membrane lipid domains reveals how cholesterol can induce lipid domain formation. *Biochemistry.* 39:843–849.

Yeagle, P. L. 1985. Cholesterol and the cell membrane. *Biochim. Biophys. Acta.* 822:267–287.

Yogev, D., A. T. Todorov, and J. H. Fendlar. 1991. Fluorescence lifetimes of diphenylhexatriene in flat and bent bilayer lipid membranes. *J. Phys. Chem.* 95:3892–3894.

Zimmerberg, J. 2000. Are the curves in all the right places? *Traffic.* 1:366–368.